ADVANCED FUNCTIONAL MATERIALS
www.afm-journal.de

Marker Pen Lithography for Flexible and Curvilinear On-Chip Energy Storage

*Qiu Jiang, Narendra Kurra, and Husam N. Alshareef**

On-chip energy storage using microsupercapacitors can serve the dual role of supplementing batteries for pulse power delivery, and replacement of bulky electrolytic capacitors in ac-line filtering applications. Despite complexity and processing costs, microfabrication techniques are being employed in fabricating a great variety of microsupercapacitor devices. Here, a simple, cost-effective, and versatile strategy is proposed to fabricate flexible and curvilinear microsupercapacitors (MSCs). The protocol involves writing sacrificial ink patterns using commercial marker pens on rigid, flexible, and curvilinear substrates. It is shown that this process can be used in both lift-off and etching modes, and the possibility of multistack design of active materials using simple pen lithography is demonstrated. As a prototype, this method is used to produce conducting polymer MSCs involving both poly(3,4-ethylenedioxythiophene), polyaniline, and metal oxide (MnO_2) electrode materials. Typical values of energy density in the range of 5–11 mWh cm^{-3} at power densities of 1–6 W cm^{-3} are achieved, which is comparable to thin film batteries and superior to the carbon and metal oxide based microsupercapacitors reported in the literature. The simplicity and broad scope of this innovative strategy can open up new avenues for easy and scalable fabrication of a wide variety of on-chip energy storage devices.

1. Introduction

The transformation of conventional electronics into flexible and curvilinear forms in various market segments has made it essential to develop on-chip energy storage devices in the similar form factor.[1,2] Currently, thin film batteries suffer from poor power density and low cycle lives, and great progress is still needed for developing miniaturized power sources.[3–6] In this scenario, microsupercapacitors (MSCs), in the form of interdigitated finger electrodes, tend to exhibit high power density as the planar configuration allows facile ionic transport with minimized values of internal resistance.[3,4] In recent years, tremendous amount of interest has been put forth in developing these planar supercapacitors employing conventional microfabrication and novel direct write techniques.

Due to its electrochemical stability, good electrical conductivity with tunable porous morphology, various forms of carbon have been explored in fabricating MSCs.[7–11] For example, activated,[7] carbide derived,[8] onion-like carbon,[9] graphene[10] and carbon nanotubes (CNTs)[11] have been patterned employing conventional photolithography and various deposition methods such as sputtering, ink-jet printing, electrophoretic, and chemical vapor deposition (CVD). Furthermore, several pseudocapacitive materials including transition metal oxides (RuO_2, MnO_2),[12,13] hydroxides ($Ni(OH)_2$),[14] and conducting polymers (polyaniline, polypyrrole and PEDOT)[15–18] have also been employed in fabricating MSCs. However, most of the reported methods involving conventional photolithography techniques which involve use of masks in a typical microfabrication protocol operated in a cleanroom environment.[7–18] In order to avoid multistep processing, complex and costly fabrication equipment, direct write innovative methods have been proposed in fabricating carbon-based MSCs. For example, laser source was used to fabricate reduced graphene oxide (rGO) MSCs by reducing graphene oxide (GO) locally.[19] EI-Kady and Kaner have demonstrated scalable fabrication of rGO MSCs by ordinary digital video disk (DVD) laser scribing technique.[20] Recently, laser-induced graphitization was employed to transform commercial polymer substrate into 3D porous graphene films for fabricating MSCs in a direct manner.[21] Printing techniques such as ink-jet printing and laser printing technologies were employed to fabricate conducting polymer-based MSCs.[22,23] Though these direct write methods have lower resolution (width and spacing between the fingers is on the order of 0.5–1 mm) than conventional photolithography-based methods, the performance of devices fabricated using these direct-write methods seems to be comparable to that of state-of-the-art thin film-based energy storage devices. However, most of the direct write techniques have been focused on fabricating carbon-based MSCs. Therefore, it is highly desirable to develop a versatile strategy in fabricating pseudocapacitive microsupercapacitors on rigid, flexible, and even curved surfaces without the need of masks, complex processing, or a cleanroom environment.

Pen is a simple, yet universal, tool that has been commonly used for writing text or drawing designs on a variety of surfaces over the years. Different types of pens can be categorized based on writing tip or point, namely ball point, roller ball, fountain, and marker. Commercially available inks can be a

Q. Jiang, Dr. N. Kurra, Prof. H. N. Alshareef
Material Science and Engineering
King Abdullah University of Science and Technology (KAUST)
Thuwal 23955-6900, Saudi Arabia
E-mail: husam.alshareef@kaust.edu.sa

DOI: 10.1002/adfm.201501698

© 2015 WILEY-VCH Verlag GmbH & Co. KGaA, Weinheim

complex medium comprising liquid or paste that contains colorants made of pigments or dyes, solvent as carrier medium, and resins as binder or glue.[24,25] Inks can be tailor designed according to the specific application requirements. Of late, it has been demonstrated that the roller ball pen filled with colloidal silver ink to write electrical conduits for developing pen-on-paper electronics.[26] Fu et al. have utilized commercial pen ink as an active material for fabricating flexible/wearable fiber-based supercapacitors.[27] They have demonstrated that the fine granular carbon particles present in the pen ink as a porous matrix for electrochemical energy storage. In contrast to the above reports, we have employed permanent or paint marker pen as a writing tool for fabricating on-chip energy storage devices on rigid, plastic, and curved platforms.

Here, we propose a simple, cost-effective, and versatile strategy to fabricate flexible and curvilinear microsupercapacitors (MSCs). The protocol involves hand-writtten sacrificial ink patterns using commercial marker pens on rigid, flexible, and curvilinear substrates. We specifically exploit the solubility contrast of the written ink patterns between aqueous and organic media, which makes it possible to deposit electroactive materials including conducting polymers and metal oxides using aqueous electrolytic baths, followed by lift-off of the ink in common organic solvents such as acetone and alcohols. We show that this process can be used in both lift-off and etching modes, also demonstrating the possibility of multistack design of active materials using simple pen lithography. As a prototype, this method was used to produce conducting polymer MSCs involving both poly(3,4-ethylenedioxythiophene), polyaniline, and metal oxide (MnO_2) electrode materials. Patterned electrochromic microcapacitors are also fabricated using the same pen lithography approach. Typical values of energy density in the range of 5–11 mW h cm^{-3} at power densities of 1–6 W cm^{-3} were achieved, which are comparable to thin film batteries and superior to the carbon and metal oxide-based MSCs reported in the literature. The simplicity and wide scope of this innovative strategy can open up new avenues for easy and scalable fabrication of a wide variety of on-chip energy storage devices.

2. Results and Discussion

Figure 1a shows an image of black, red, and blue permanent markers, which are water proof as their ink is unaffected by the humid environment. Typical design of a marker pen includes the tip inserted at its head, and an ink barrel loaded in a plastic casing. As shown in Figure 1b, the writing color of the marker pen is decided by the choice of pigment filled in the ink barrel.[24,25] Tip of the marker is a long stick which is porous and sponge-like material, protruding slightly out as shown in

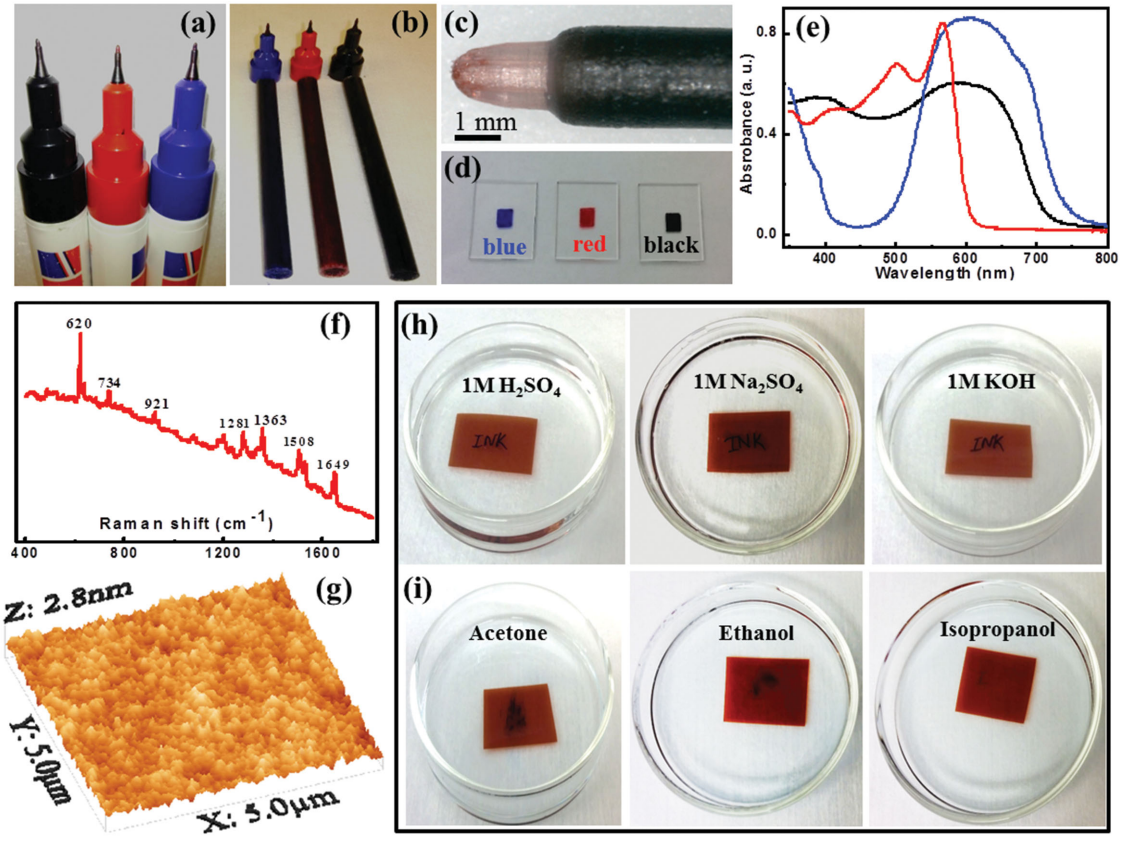

Figure 1. Digital photographs showing a) black, red, and blue marker pens, b) their heads and ink barrels. c) Optical image of fibrous tip of the marker. d) Painting of blue, red, and black colored boxes on glass. e) UV–vis absorption spectra of ink films, shown with their respective colors. f) Raman spectrum and g) AFM topography of the red ink mark. Photographs showing the solubility contrast of the "INK" mark on a plastic polyimide sheet h) in aqueous acidic, neutral and basic media versus i) organic media.

© 2015 WILEY-VCH Verlag GmbH & Co. KGaA, Weinheim

Figure 1c. Three square boxes were filled by sketching with blue, red, and black colored ink marks on glass substrates as shown in Figure 1d. The corresponding UV–vis absorption spectra of these colored films are shown in Figure 1e, which exhibit broad absorption bands covering the entire visible range. This kind of absorption characteristics is typical of phthalocyanine-based pigments as they are being used in the commercial marker pens to impart desired colors (spectra are shown with the respective colors of the ink, see Figure 1e).[24,25] Further, in order to probe the UV absorption characteristics of these pigments, solutions of different colored (black, red, and blue) inks were made by dissolving the inks in ethanol solvent, and their characteristic UV–vis absorption spectra were recorded (see Figure S1, Supporting Information). The UV absorption characteristics are seen to be different for blue, red, and black colored solutions, as expected for different types of pigments. In order to probe the skeletal vibrations of pthalocyanine, we have employed 785 nm laser excitation to record the Raman spectrum of red ink mark as shown in Figure 1f. The characteristic Raman peaks at 1649 cm^{-1} can be ascribed to skeletal vibration of porphyrin ring system (from pigment of phthalocyanine), 1508, 1363 cm^{-1} correspond to C═C and C═N skeletal vibrations, band at 1281 cm^{-1} corresponds to C—H bending and stretching of porphyring ring, 1202 cm^{-1} is due to C—C stretch in porphyrin ring and 620 cm^{-1} corresponds to C—H out-of-plane deformation of phenyl unit.[28] Further, AFM imaging was done on the ink mark to estimate the surface roughness and topography. 3D AFM topography image of ink is shown in Figure 1g with quite smooth surface morphology with an rms roughness of 0.2–0.3 nm, which is remarkably good for a hand-drawn pattern (see Figure S2, Supporting Information).

As colorant dyes are water soluble, pigments are usually added to the ink of a permanent marker which is resistant to dissolution by humid and other environmental agents (see Figure 1d). Unlike permanent marker inks, water-based inks can easily be erased by water itself as shown in Figure S3, Supporting Information. However, we found that permanent ink patterns were unaffected by aqueous media such as 1 M H_2SO_4, 1 M Na_2SO_4, 1 M KOH as shown in Figure 1h. The ink of the permanent marker also includes fast drying and less toxic solvents such as alcohols, which play the role of liquid carrier to dissolve and transport ink colorant and resins through the fibrous sponge. Ink resin is typically a glue-like polymer such as polyamide, acrylic, rosin, or phenolic which improves adhesion of the colorant pigment to surfaces after solvent evaporation. We have discovered that the permanent ink marker pattern can be erased by organic solvents such as acetone, ethanol, and isopropanol, as shown in Figure 1i. This kind of solubility contrast of the ink toward aqueous and organic media resembles that of photoresist at the stages of development (done by aqueous bath) and lift-off (done by organic solvents). Hence, permanent marker ink was used to define sacrificial pattern for depositing metal layers by sputtering and electrochemical deposition of conducting polymers using aqueous acid medium as supporting electrolyte (1 M H_2SO_4). At the final stage, lift-off using ethanol was performed to erase off ink patterns to define the interdigitated conducting polymer electrodes. Even, we have done selective electrodeposition of active materials after lift-off while not having shorting paths at a typical electrode spacing of 0.5 mm.

The typical diameter of the tip of marker pens is around 0.8 mm. The pattern width (0.3–1 mm) is governed by the wettability of the ink on a given surface, force and speed of writing (see the Supporting Information, Figure S2).[26] Fast drying inks can avoid the smearing of written features on a given surface through instant evaporation of solvent present in the ink up on writing. Writing of ink patterns was done on various commonly used substrates such as printing paper, plastic substrates such as polyethylene terephthalate (PET), polyethylene naphthalate (PEN), polyimide (PI), rigid substrates including glass and SiO_2/Si and even on curved platforms such as glass vial, pipe, and cable. Lift-off protocol using ink patterns allows us to fabricate microsupercapacitors on both flat and curved surfaces. For example, the schematic shown in **Figure 2**a illustrates the process flow in fabricating in-plane microsupercapacitors over a flat surface. Initially, plastic PEN sheet was used as a substrate to draw the desired patterns using marker pen, followed by Au metal deposition. Repeated tests confirmed that the ink lift-off process using ethanol removes the ink pattern while retaining the Au metal in the form of interdigitated fingers (see the Supporting Information, Figure S4). As this ink pattern is unaffected by aqueous media (see Figure 1h), we used aqueous electrolytic baths for depositing porous conducting polymer film before the lift-off (see the Supporting Information, Figure S5).

In principle, various active materials such as carbon, metal oxides/hydroxides can also be deposited by painting, sputtering, and electrochemical deposition, as long as the process is based on aqueous solutions or suspensions (see the Supporting Information, Figure S6). The final step of lift-off in organic solvents such as ethanol and isopropanol would result in the clean and neat conducting polymer interdigitated finger electrodes. This kind of writing using a marker pen not only restricts us in writing over flat surfaces but also over curved surfaces such as glass vials, pipes, and cables. Following the lift-off protocol described above, we could successfully fabricate microsupercapacitors on flat and curvilinear platforms as shown in the inset of Figure 2a. Certainly, our technique has the potential in fabricating energy storage units over curvilinear platforms which is clearly a novel aspect when compared to conventional microfabrication techniques.

The versatility of this technique was also demonstrated in fabricating electrochromic microsupercapacitors employing etching protocol. In a typical process, we have used ink layout as a masking pattern to selectively etch thin films for obtaining finger patterns. To demonstrate the etching process, indium tin oxide (ITO) thin film on glass was written with interdigitated ink pattern using a paint marker as shown in Figure 2b. Unmasked regions of ITO were etched away using 3:1 HCl:H_2O for 4 min. After the etching process, ITO surface is thoroughly washed in DI water followed by drying by blowing N_2 gas. Finally, the ink pattern was removed by dissolving in ethanol to obtain transparent interdigitated ITO fingers. These conducting transparent ITO patterns were coated with thin films (<200 nm) of conducting polymer by electrodeposition. Further, the electrochromic nature of conducting polymer patterns was visualized upon charging/discharging of the MSC (ion gel electrolyte) as shown in Figure 2c. The color change of the respective conducting polymer finger electrodes can be attributed to the doping/dedoping processes during charging/discharging

© 2015 WILEY-VCH Verlag GmbH & Co. KGaA, Weinheim

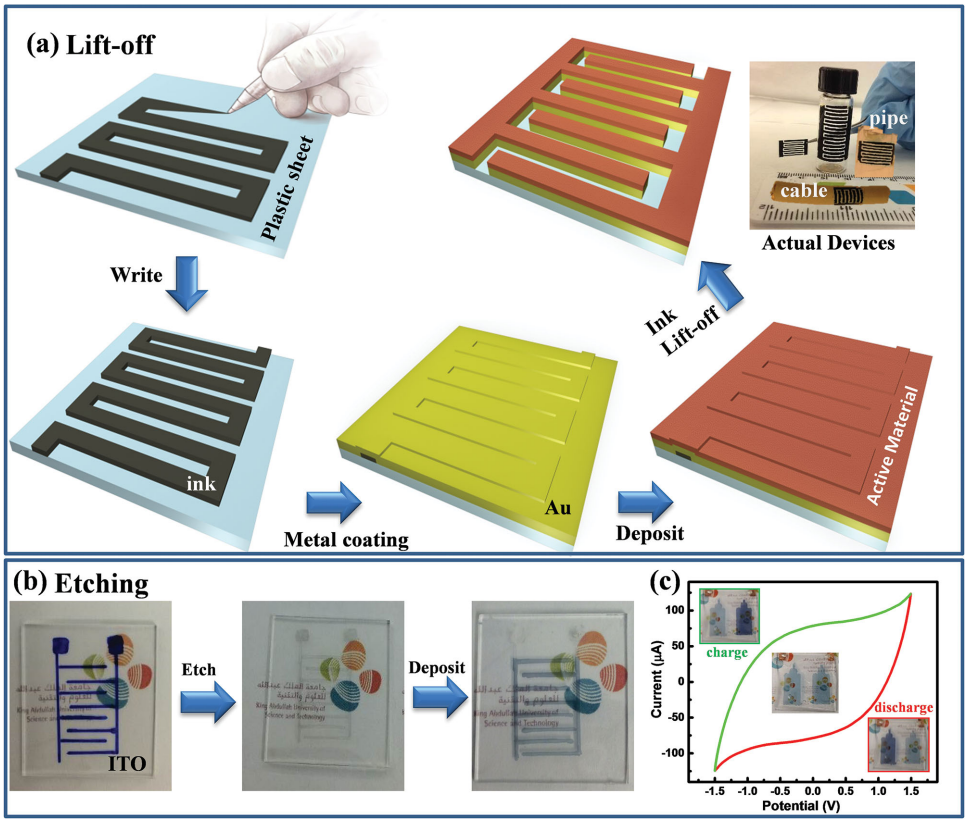

Figure 2. a) Schematic illustrating the process flow sequence for fabricating in-plane microsupercapacitors, starts with writing an ink pattern using a marker pen over a plastic sheet, metal coating, deposition of conducting polymer and then lift-off ink pattern in organic solvents to obtain interdigitated conducting polymer finger electrodes (arrows are shown as guidance). Inset photograph showing the microsupercapacitors fabricated over flat and curved surfaces including glass vial, pipe, and cable. b) Selective etching of ITO surface using ink pattern as a protecting layer, followed by removal of ink using ethanol and depositing thin conducting polymer over the ITO fingers. c) CV curve of electrochromic PEDOT MSC, inset photographs show neutral, charged, and discharged states of PEDOT MSC.

events. Therefore, this technique is quite simple yet versatile enough to fabricate planar, curvilinear, and electrochromic microsupercapacitors.

To demonstrate the viability of this technique, we have chosen aqueous electrolytic baths in electrodepositing conducting polymers or metal oxides over the interdigitated conducting tracks. Anodic potential oxidizes the EDOT monomers to deposit PEDOT films over the Au surface as shown in **Figure 3**a. This nanostructured porous PEDOT film can facilitate faster ionic transport resulting in improved electrochemical performance. As shown in the inset of Figure 3a, the deposition of PEDOT is uniform over the Au fingers, and remains intact even after rigorous ultrasonication during the lift-off step. The strong adherence of PEDOT to the Au current collector and its porous morphology can aid in reducing charge transfer resistance across the electrolyte/electrode interface. The typical width and interspace between the fingers was found to be 500 ± 50 and 450 ± 50 μm. Since manual drawing would result in the variation of geometric parameters of the MSC devices, we have investigated the electrochemical performance of three different devices with similar geometric parameters (width = 500 ± 50 μm, spacing = 450 ± 50 μm) and data are shown in the Supporting Information, Figure S8. The thickness of the PEDOT films was controlled through deposition time. The thickness of PEDOT was found to be 200 nm for 1 min deposition, and gradually increased up to 1.9 μm for deposition time of 15 min (see the Supporting Information, Figure S7). Further, the role of geometric parameters of the electrodes as well as the thickness of the active materials toward the electrochemical performance was investigated. It was observed that lower the spacing, higher is the electrochemical performance, due to reduced pathway for the ion migration (see the Supporting Information, Figure S9).

Further, the Raman spectra of electrodeposited PEDOT were compared to that of commercial PEDOT:PSS films as shown in Figure 3b. Indeed, electrodeposited PEDOT film (red curve) shows similar characteristic peaks as that of commercial PEDOT:PSS films (black curve). As PSS is a weak Raman scatterer, all these peaks are assignable to the various normal modes of vibration of atoms present in the PEDOT chains. The bands at higher wavenumbers such as 1573, 1503 cm^{-1} could be assigned to asymmetric stretching of Cα=Cβ while the most intense peak at 1441 cm^{-1} relates to symmetric stretching of Cα=Cβ. The peak at 1441 cm^{-1} may also provide information related to doping and dedoping in PEDOT chains. The peak at 1367 cm^{-1} corresponds to Cβ–Cβ interring stretching, 1264 cm^{-1} represents Cα–Cα interring stretching, 1105 cm^{-1} is due to C–O–C deformation, 988 cm^{-1} represents C–C antisymmetrical

© 2015 WILEY-VCH Verlag GmbH & Co. KGaA, Weinheim

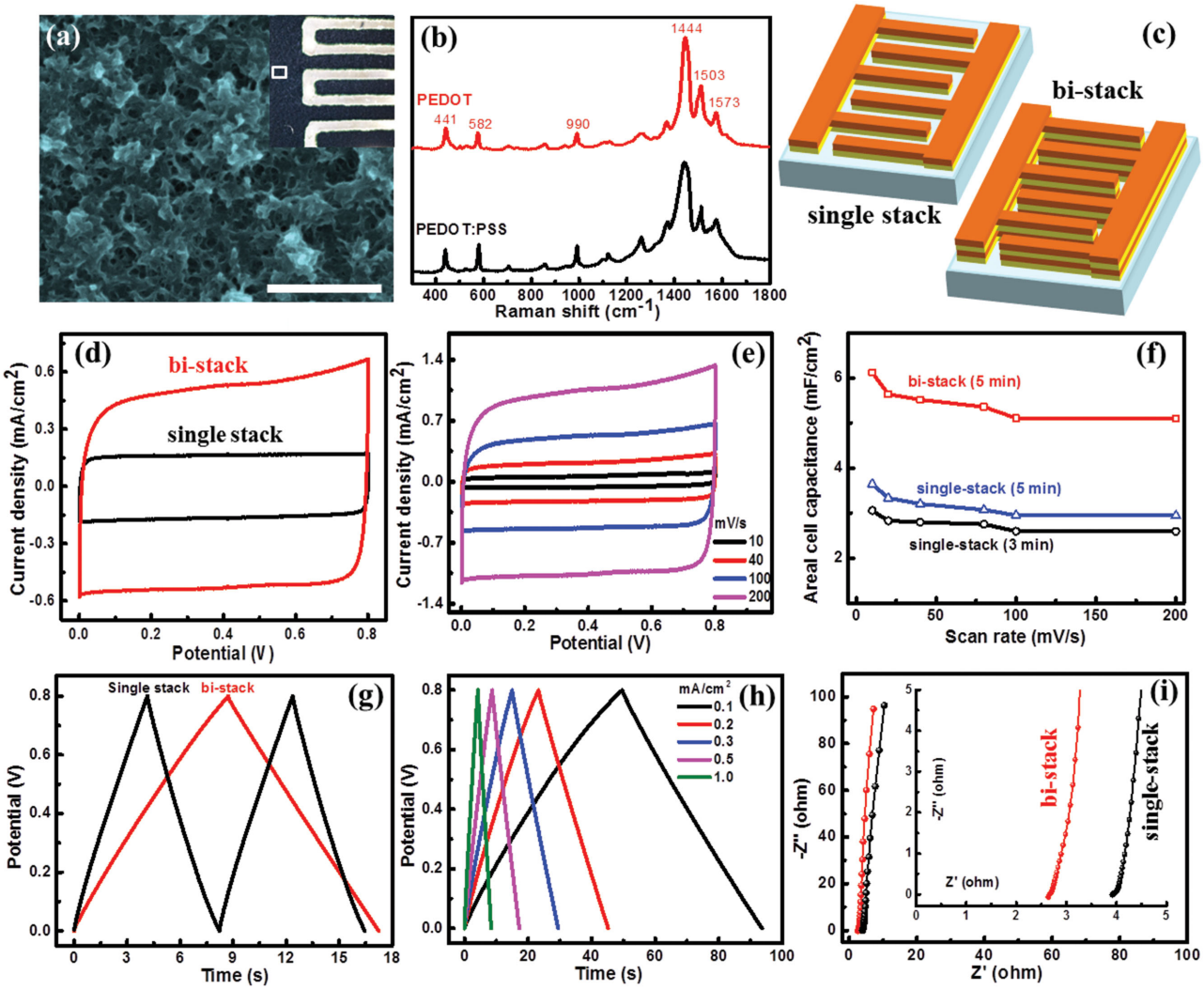

Figure 3. a) SEM image of nanostructured PEDOT, inset shows the optical image of PEDOT/Au interdigitated finger electrodes. b) Comparative Raman spectra of electrodeposited PEDOT (red curve) and commercial PEDOT:PSS (black curve). c) Schematic showing the single and bistacks of PEDOT/Au. d) Comparison of CVs of bi-stack:PEDOT/Au/PEDOT/Au with single stack:PEDOT/Au at a scan rate of 100 mV s^{-1}. e) CVs of bistack of PEDOT/Au MSC at different scan rates. f) Comparison of areal cell capacitance of bi-stack with respect to single stacks. CDs of g) single-stack versus bistack at a current density of 0.5 mA cm^{-2} and h) bi-stack PEDOT/Au MSC at different current densities. i) Nyquist spectra of bi-stack and single-stack PEDOT/Au MSCs, inset is the high-frequency region of the spectra.

stretching mode, 702 cm^{-1} corresponds to symmetric C—S—C deformation, 573 cm^{-1} is due to oxy-ethylene ring deformation, and 441 cm^{-1} corresponds to SO_2 bending, confirms the doping of sulfate and bisulfate anions (from sulfuric acid) in PEDOT nanostructures during the electrochemical deposition.[29]

The versatile nature of the pen lithography was explored in fabricating vertical bistack of PEDOT/Au heterostructures. After fabricating the single stack MSC which comprises PEDOT (2 min)/Au interdigitated electrodes, ink pattern was drawn in the interspacings using marker pen followed by depositing second layer of Au with subsequent electrochemical deposition of PEDOT for 3 min. Thus, we have found that fabricating vertical bistack of PEDOT/Au was quite easy employing this technique (see Figure 3c, see the Supporting Information, Figure S10). Fabricating a second layer on top of porous conducting polymer surface may be a tricky aspect in a conventional photolithography process. Moreover, during the second layer of fabrication, photoresist gets trapped into the porous matrix of active material (in this case porous PEDOT), that may suppress the electrochemical active surface area. As in the case of pen lithography, ink pattern was drawn only in the interspaces while not affecting the porous PEDOT surface sites, helping us building vertical stacks that can retain their electrochemical attributes. Interestingly, the areal capacitance of vertical bi-stack of PEDOT/Au was found to be almost twice that of single stack of PEDOT/Au (tested in a two-electrode configuration, 1 M H_2SO_4) as shown in Figure 3d. Further, CV scans of vertical bi-stack PEDOT/Au MSC were recorded at different scan rates as shown in Figure 3e. At a scan rate of 10 mV s^{-1}, vertical bi-stack PEDOT (3 min)/Au/PEDOT (2 min)/Au exhibits an areal capacitance of 6 mF cm^{-2} which is almost twice that of single stack of PEDOT (3 min)/Au and 1.5 times higher than single-stack

© 2015 WILEY-VCH Verlag GmbH & Co. KGaA, Weinheim

PEDOT (5 min)/Au MSC (see Figure 3f). As shown in Figure 3g, discharge time of bi-stack PEDOT/Au MSC is almost twice that of single stack at a current density of 0.5 mA cm^{-2}. Charge–discharge curves of bistack PEDOT/Au MSC were recorded at different current densities as shown in Figure 3h. Impedance spectra are seen parallel to the Z'' axis for the single and bi-stack PEDOT/Au MSCs, indicating that excellent capacitive behavior (see Figure 3i). Absence of semicircle in the high-frequency region for both the single and bistack devices signifies that negligible charge-transfer resistance. However, as shown in the inset of Figure 3i, bistack MSC exhibits a lower value of equivalent series resistance (ESR), 2.6 Ω when compared to single-stack with ESR of 3.9 Ω. Thus, introducing the Au layer improves the conductivity of PEDOT that subsequently causes the enhanced values of areal capacitance for the vertical bi-stack PEDOT/Au MSC. Therefore, this technique has a potential in building vertical stacks of conducting polymer/metal MSCs for improving the electrochemical performance.

Since liquid electrolyte has a tendency for leakage with improper encapsulation or sealing, gels electrolytes are preferred to fabricate leakage-free solid-state conducting polymer MSCs. Due to higher electrochemical potential window (>1 V) of ion gel electrolytes, MSCs can exhibit superior energy ($E = ½\ CV^2$) and power densities ($P = V^2/4R$) over aqueous media. As PEDOT is electroactive in a wide potential window (up to 1.4 V) while having electrochemical activity in various media (aqueous, organic, and ionic liquid), ion gel based PEDOT MSCs were fabricated on flexible and curved surfaces. A thin layer of ion gel (thickness of 30 µm) was drop-coated over the interdigitated PEDOT finger electrodes followed by drying off completely. Cyclic voltammograms of PEDOT MSC using ion gel electrolyte were recorded at various scan rates from 100 mV s^{-1} to 5 V s^{-1} (see **Figure 4**a). CV curves are seen typical of rectangular in the potential window of 1.5 V unlike aqueous media of 0.8 V. CD profiles are seen quite linear in the potential window of 0–1.5 V at different current densities (1–8 A cm^{-3}) as shown in Figure 4b. As these PEDOT MSCs were fabricated on a flexible substrate, the device can be bent and released for several times without destroying it. Further, we have tested the flexibility of the device by measuring its CV before and after bending as shown in Figure 4c. CV curves remain the same for the normal (shown with black curve) and bending (red curve) configurations of this device as shown in Figure 4c.

Furthermore, we take the advantage of writing ink pattern over curved surfaces in fabricating MSCs on curvilinear platforms (see Figure 4d). In order to meet the desired power capability, tandem configuration of MSCs such as series and parallel combinations was made to increase the voltage and current ratings, respectively. Two cells connected in parallel exhibit enhanced current values over a single cell (see Figure 4e). As shown in Figure 4f, two MSCs fabricated on a curved glass surface were connected in series to increase the cell potential up to 3 V when compared to single cell of 1.5 V. CV curves shown in Figure 4d reveal that the current values of series connected devices decrease at the expense of increased potential window. Cycling stability of this PEDOT MSC was tested over 20 000 cycles by continuous charging and discharging between 0 and 1.5 V in ion gel electrolyte. Indeed, this solid-state MSC exhibits good cycling stability with a capacitance retention up to 85% and coulombic efficiency of 95% over 20k cycles as shown in Figure 4g. Series-connected PEDOT

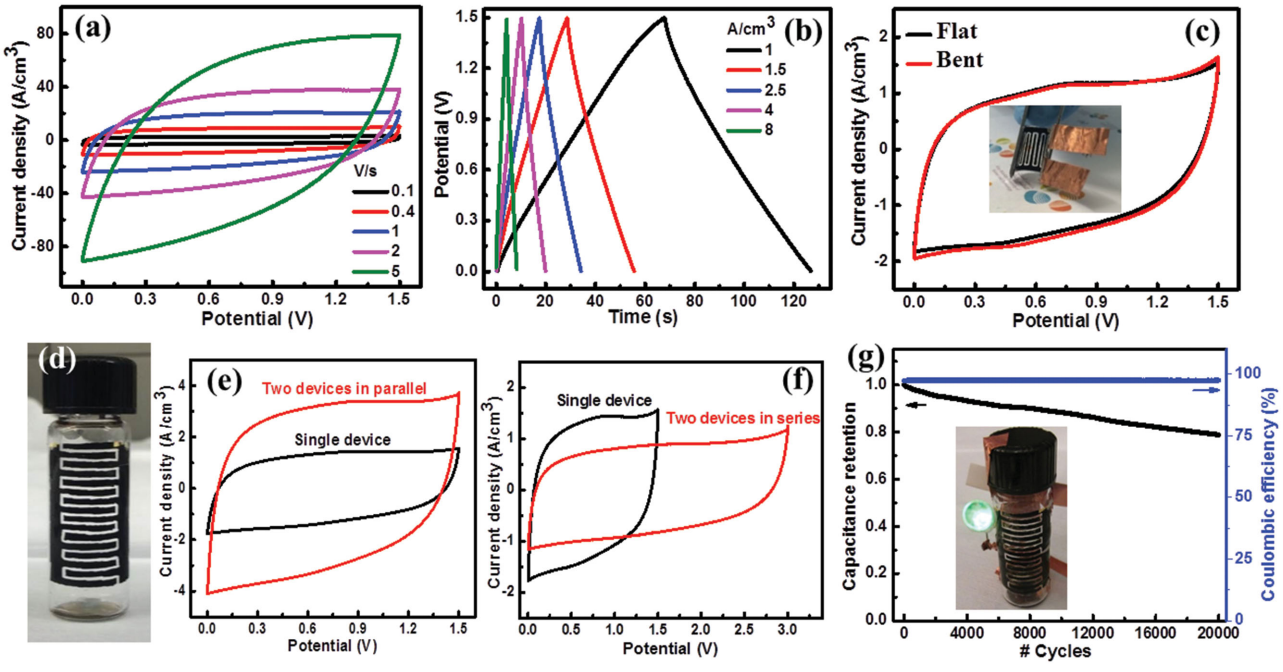

Figure 4. a) CVs and b) CDs of PEDOT MSCs using ion-gel electrolyte. c) CV curves for the flat (black) and bent (red curve) PEDOT MSC employing ion-gel electrolyte at a scan rate of 80 mV s^{-1}, inset shows the digital photograph for the bent configuration of PEDOT MSC. d) Digital photograph showing the PEDOT MSC over a curved glass vial. CVs of PEDOT MSCs in e) parallel and f) series combinations at a scan rate of 80 mV s^{-1}. g) Cycling stability and Coulombic efficiency of PEDOT MSC over 20 000 cycles in ion-gel electrolyte. Inset shows MSCs fabricated over curved substrate as a power source in glowing green LED.

© 2015 WILEY-VCH Verlag GmbH & Co. KGaA, Weinheim

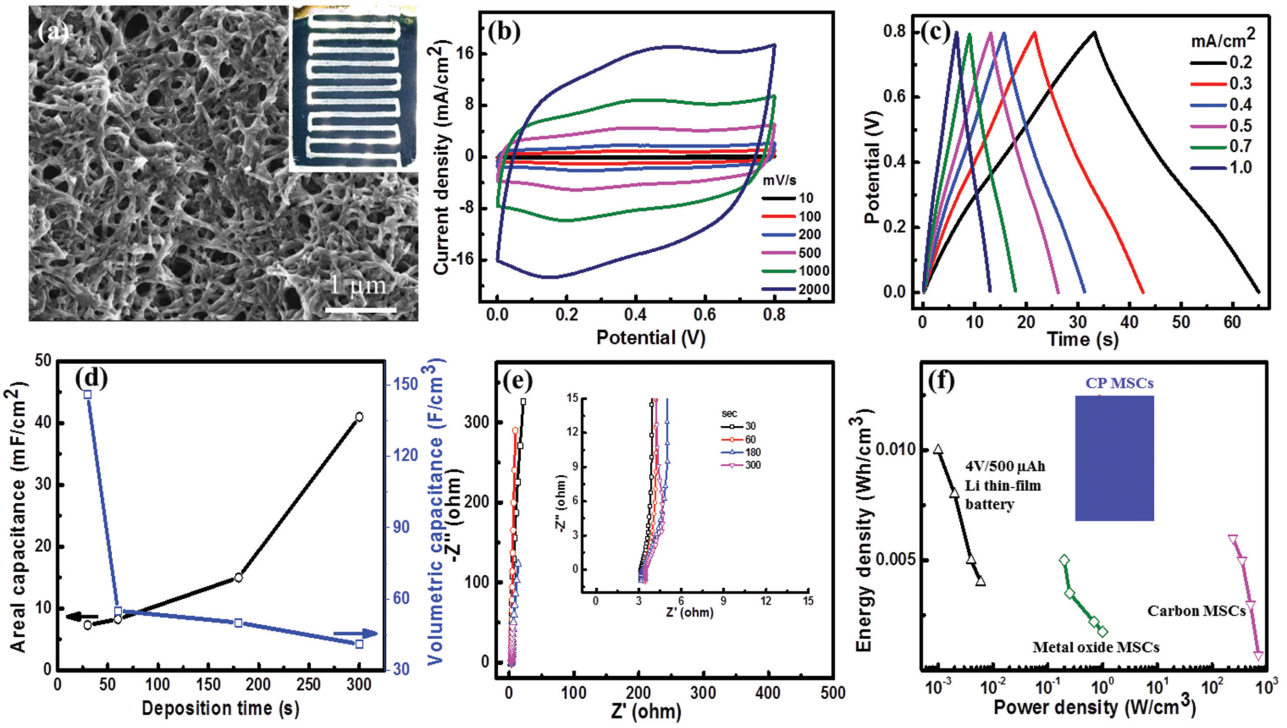

Figure 5. a) SEM morphology of PANI nanofiber network, inset showing the optical image of PANI MSC. b) CVs and c) CDs of PANI MSC in PVA/H_2SO_4 gel electrolyte. d) Variation in the areal and volumetric capacitances of PANI MSCs with deposition time. e) Nyquist spectra of various PANI MSCs, inset shows the high-frequency region of spectra. f) Ragone plot showing the energy and power density of Li thin-film batteries, carbon and metal oxide based MSCs with respect to conducting polymer based MSCs fabricated in this study.

MSCs on a curved glass surface were initially charged using a battery. Inset photograph shows the tandem PEDOT MSCs fabricated over a curved surface are capable as a stand-alone micropower source in glowing a green light emitting diode. Thus, this pen lithography technique can allow us to fabricate curvilinear energy storage platforms as micropower units that may be compatible with curvilinear electronics.

Further, in order to generalize this technique, we have electropolymerized high capacity conducting polymer, polyaniline in the form of nanofiber network as shown in **Figure 5**a. The uniform and homogenous growth of PANI nanofiber network over the Au fingers is evident from the optical image shown in the inset of Figure 5a. The electrochemical performance of PANI MSC was tested in PVA/H_2SO_4 gel electrolyte in a two-electrode configuration. CV curves of PANI MSC exhibit broad redox peaks due to Faradaic nature of PANI nanofiber network (see Figure 5b). At a scan rate of 40 mV s^{-1}, PANI solid-state device exhibits an areal capacitance of 26 mF cm^{-2}. Indeed, this value is comparable to the values reported in the literature based on PANI MSCs fabricated by photolithography and laser printing techniques.[16,23] Similarly, charge–discharge profiles are seen with curvature, due to pseudocapacitive nature of PANI MSC (see Figure 5c). Variation in areal and volumetric cell capacitances of PANI MSCs with different deposition times is shown in Figure 5d. Areal cell capacitance is gradually increasing from 7.3 to 41 mF cm^{-2} as the deposition time is increased from 30 s to 5 min. However, the volumetric capacitance was found to be maximum of 146 F cm^{-3} for 0.5 μm thick PANI. Nyquist spectra of various PANI MSCs are seen vertical, indicating good capacitive behavior of the fabricated devices (see Figure 5e). In the high-frequency region of the spectra, a small semicircle is observed for all the PANI MSCs which is due to charge-transfer resistance across the electrode/electrolyte interface (see inset of Figure 5e). All these PANI MSCs exhibit an equivalent series resistance (ESR) of 3 Ω as shown in the inset of Figure 5e. Cycling stability of PANI MSC was tested in PVA/H_2SO_4 gel electrolyte over 5000 cycles (see the Supporting Information, Figures S11 and S12). Ragone plot displayed in Figure 5f compares the electrochemical performance of conducting polymer-based MSCs with the state-of-the-art energy storage devices.[30,31] These CP-based MSCs (PEDOT-ion gel and PANI-aqueous gel) exhibit volumetric energy density values in the range of 5–11 mWh cm^{-3} and power densities in the range of 1–6 W cm^{-3}. Thin PANI deposits (thickness, 500 nm) exhibit maximum volumetric capacitance and hence a maximum energy density of 12 mWh cm^{-3} was achieved. There have been quite a few reports on PANI MSCs employing electrochemical deposition, dilute polymerization techniques to achieve high-energy density.[15,16,23] In fact, PEDOT MSC with thickness of 1.2 μm in ion gel electrolyte exhibits a maximum energy density of 9 mWh cm^{-3}. The excellent electrochemical stability of PEDOT among the other conducting polymers led us to explore in building vertical stacks and curvilinear energy storage platforms in a more reliable manner.

It is worth mentioning a few merits and demerits of this technique at this stage. Though the feature widths and spacing obtained are higher compared to microfabrication process, given its simplicity and versatility, it is a unique technique with a wide

© 2015 WILEY-VCH Verlag GmbH & Co. KGaA, Weinheim

scope for on-chip energy storage. Fabrication of MSCs on curved surfaces is clearly a novel aspect of this technique which is otherwise not possible by means of conventional photolithography. Although these devices were fabricated manually, in principle one can automate this maskless process to make microsupercapacitors over any kind of curved surface with excellent precision and at low cost. Given the simplicity of the process, it can be used to fabricate microsupercapacitors in a variety of designs. Thus, this method opens up a new avenue in fabricating on-chip energy storage devices over curved surfaces, a field of *curvilinear energy storage*. However, implementation of this technique in industrial production could demand for certain level of sophistication. For example, these manual drawings can be automated by employing robotic arms or plotters to control geometric parameters precisely in order to attain more reliable and reproducible performance.

This method can be extended in terms of achieving high resolution and scalability through design of functional inks by following soft lithography approaches. For example, PDMS stamps can be used to print or mold the ink patterns with a typical resolution less than 0.1 mm easily. In this case, PDMS stamps have to be predesigned employing photolithography technique. This method can be extended in terms of achieving high resolution and scalability through design of functional inks by following soft lithography approaches.[32] By designing the PDMS stamps with a desired resolution, one can use these inks to get printed or molded as sacrificial patterns in fabricating microsupercapacitors with high resolution. Further, a great variety of functional inks based on various electroactive materials (carbon, metal oxides, conducting polymers) can also be developed to fabricate printed microsupercapacitors. Alternatively, one can use plotters/printers (ink-jet and sonplot) in dispensing the sacrificial ink patterns in a reliable manner for large area patterning with better reproducibility. A great variety of inks based on various active materials can be developed to fabricate printed microsupercapacitors. The ultimate goal is to develop scalable, high-resolution printing technology for integrating electronic devices with energy storage units.

3. Conclusions

A simple and versatile strategy was demonstrated for fabricating on-chip energy storage devices employing sacrificial ink patterns written by commercial marker pens. This technique was used to fabricate microsupercapacitors over a wide variety of substrates including rigid, flexible, and even curved surfaces without difficulty. We have successfully demonstrated both lift-off and etching schemes of this technique to realizing flexible, curved, and electrochromic microsupercapacitors. As this technique does not use masks, we have shown that it can be used to make vertical stacks of multilayer structures without using sophisticated optical aligning equipment.

4. Experimental Section

Materials: Chemicals were used as received without further purification. Analytical grade H_2SO_4, Aniline (Ani) and 3,4-ethylenedioxythiophene (EDOT), $Mn(NO_3)_2$, and surface active reagent sodium dodecyl sulfate (SDS, $CH_3(CH_2)_{11}OSO_3Na$) were purchased from Sigma-Aldrich. Polyvinyl alcohol (PVA), poly(vinylidene fluoride-*co*-hexafluoropropylene), P(VDF-HFP) with M_n = 130 000 Da and 1-Ethyl-3-methylimidazolium bis(trifluoromethylsulfonyl)imide, [EMIM][TFSI] were purchased from Sigma-Aldrich.

Pen Lithography to Fabricate Microsupercapacitors: Plastic polyethylenenaphthalate (PEN) substrates (thickness, 125 μm) were employed as platforms in order to fabricate microsupercapacitor devices. Flexible and rigid substrates such as printing paper, polyimide (PI), polyethylene terephthalate (PET), glass (borosilicate), ITO/glass were used as platforms in fabricating microsupercapacitors. Ordinary glass vials, pipes, and cables were used as curved surfaces in fabricating curvilinear microsupercapacitors. Permanent (Edding 404, stroke width of 0.75 mm) and paint markers (Edding 780, stroke width of 0.8 mm) were bought from Edding Products. The ink present in these markers was water proof with different colors depending on the presence of type of pigment. Patterns of interest were drawn on various surfaces by hand using a ruler paper as a guide. The width of interspace was dependent upon force and speed of writing which ranges from ≈0.5 to 1 mm. Typical area of the devices was around 1 cm^2. Ink pattern was drawn to obtain interdigitated patterns followed by coating metal layers such as 150 nm Au/20 nm Ti and electrodepositing conducting polymers. Before the lift-off process, different conducting polymers (PEDOT and Pani) were electrodeposited in a standard three-electrode configuration in a glass cell consisting Au coated chips as working electrode, a platinum wire as a counter electrode, and Ag/AgCl as a reference electrode at room temperature. The electrolyte solution containing equimolar ratio EDOT and SDS (10^{-3} M) in 1 M H_2SO_4 using CHI 660 D Electrochemical Workstation at a constant anodic potential of 0.9 V (vs Ag/AgCl) for different times.[33] Electrolytic bath for PANI involves 0.5 M Aniline with 1 M H_2SO_4 as a supporting electrolyte, first step of nucleation by applying constant potential of 0.85 V for 1 min followed by growing nanofibers by applying constant current of 5 mA cm^{-2} for different times.[34] The electrochemical deposition of MnO_2 was carried out by employing 10×10^{-3}M of $Mn(NO_3)_2$ with 50×10^{-3} M of $NaNO_3$ as a supporting electrolyte.[35] Galvanostatic deposition technique with a constant current density of 0.5 mA cm^{-2} was applied using an electrochemical workstation. After the electrochemical deposition, the samples were thoroughly washed with DI water in order to remove any surfactant molecules or monomer adsorbed on the surface.

Material Characterization: Surface morphology and microstructure were imaged by scanning electron microscope (SEM) (Nova Nano 630 instrument, FEI Co., The Netherlands). The film thicknesses were measured using a Veeco Dektak 150 surface profilometer. Raman spectroscopy measurements were carried out on the PEDOT and PANI samples using a micro-Raman spectrometer (LabRAM ARAMIS, Horiba-Jobin Yvon). Raman spectra acquired with notch filters cutting at 100 cm^{-1} using a cobalt laser (473 nm, 5 mW at source) and a laser spot size of 1.5 μm for CPs. For ink markers, we had laser excitation wavelength of 785 nm with acquisition time of 60 s using appropriate filters to avoid the damage due to laser induced heating. AFM imaging was done on an Asylum AFM (MFP-3D) using Si probes (model RTESPA, spring constant 40 N m^{-1}) in tapping mode. AFM 3D and roughness analysis was done using WSxM software 4.0 Beta 7.0.[36]

Preparation of Liquid and Polymer Gel Electrolytes: The electrochemical properties of the PEDOT films were investigated in a two-electrode configuration in 1 M H_2SO_4. The PVA/H_2SO_4 gel electrolyte was prepared as follows: 1 g of H_2SO_4 was added into 10 mL of deionized water, followed by 1 g of PVA powder. The whole mixture was heated to 85 °C while stirring until the solution became clear. Ionic gel electrolyte was prepared by dissolving 0.5 g of P(VDF-HFP) in 5 mL of acetone followed by adding 1.3 mL of ionic liquid, [EMIM] [TFSI] while stirring. The typical thickness of the polymer–electrolyte was around 30 μm.

Electrochemical Characterization of Microsupercapacitor Devices: All the electrochemical measurements were performed in the two-electrode configuration as it was more relevant when the practical applications were concerned. As the deposited material was of very tiny amounts,

© 2015 WILEY-VCH Verlag GmbH & Co. KGaA, Weinheim

gravimetric capacitance might not be accurate in this case. Hence, the areal cell and volumetric capacitance of the microsupercapacitor devices were calculated by taking the total area and volume of the electroactive electrodes into consideration. Solid-state supercapacitor devices were fabricated by applying the polymer gel electrolyte over the conducting polymer interdigitated finger electrodes followed by drying the excess water in dry air. Cyclic voltammetry (CV), galvanostatic charge–discharge (CD), electrochemical impedance spectroscopy (EIS), and electrochemical cycling stability were performed using VMP3 multichannel electrochemical workstation (Bio-Logic). The CVs were tested in a voltage window between 0 and 0.8 V over a wide range of scan rates. The CDs were measured in the same voltage window under a wide range of current densities. The electrochemical impedance spectroscopy (EIS) was measured using a Modulab (Solartron Analytical) electrochemical workstation in the frequency range from 100 kHz to 0.01 Hz at open circuit potential by applying a small sinusoidal potential of 10 mV signal. All measurements were carried out at room temperature.

Supporting Information

Supporting Information is available from the Wiley Online Library or from the author.

Acknowledgements

Q.J. and N.K. contributed equally to the work. Research reported in this publication was supported by King Abdullah University of Science and Technology (KAUST). The authors thank the Advanced Nanofabrication, Imaging and Characterization Laboratory at KAUST for their excellent support. The authors thank Dr. Pradipta Nayak for useful discussions. N.K. acknowledges the support from SABIC Postdoctoral Fellowship.

Received: April 27, 2015
Revised: June 6, 2015
Published online: July 14, 2015

[1] D.-H. Kim, J. Xiao, J. Song, Y. Huang, J. A. Rogers, *Adv. Mater.* **2010**, *22*, 2108.
[2] D.-H. Kim, J. Song, W. M. Choi, H.-S. Kim, R.-H. Kim, Z. Liu, Y. Y. Huange, K.-C. Hwang, Y.-W. Zhang, J. A. Rogers, *Proc. Natl. Acad. Sci. USA* **2008**, *105*, 18675.
[3] M. Beidaghi, Y. Gogotsi, *Energy Environ. Sci.* **2014**, *7*, 867.
[4] G. Xiong, C. Meng, R. G. Reifenberger, P. P. Irazoqui, T. S. Fisher, *Electroanalysis* **2014**, *26*, 30.
[5] J. W. Long, B. Dunn, D. R. Rolison, H. S. White, *Chem. Rev.* **2004**, *104*, 4463.
[6] D. R. Rolison, R. W. Long, J. C. Lytle, A. E. Fischer, C. P. Rhodes, T. M. McEvoy, M. E. Bourga, A. M. Lubers, *Chem. Soc. Rev.* **2009**, *38*, 226.
[7] D. Pech, M. Brunet, P. L. Taberna, P. Simon, N. Fabre, F. Mesnilgrente, V. Con´ed´era, H. Durou, *J. Power Sources* **2010**, *195*, 1266.
[8] J. Chmiola, C. Largeot, P. L. Taberna, P. Simon, Y. Gogotsi, *Science* **2010**, *328*, 480.
[9] D. Pech, M. Brunet, H. Durou, P. Huang, V. Mochalin, Y. Gogotsi, P.-L. Taberna, P. Simon, *Nat. Nanotechnol.* **2010**, *5*, 651.
[10] Z. S. Wu, K. Parvez, X. Feng, K. Müllen, *Nat. Commun.* **2013**, *4*, 2487.
[11] J. Lin, C. Zhang, Z. Yan, Y. Zhu, Z. Peng, R. H. Hauge, D. Natelson, J. M. Tour, *Nano Lett.* **2012**, *13*, 72.
[12] T. M. Dinh, K. Armstrong, D. Guay, D. Pech, *J. Mater. Chem. A* **2014**, *2*, 7170.
[13] W. Si, C. Yan, Y. Chen, S. Oswald, L. Han, O. G. Schmidt, *Energy Environ. Sci.* **2013**, *6*, 3218.
[14] N. Kurra, N. A. Alhebshi, H. N. Alshareef, *Adv. Energy Mater.* **2014**, *4*, 1401303.
[15] K. Wang, W. Zou, B. Quan, A. Yu, H. Wu, P. Jiang, Z. Wei, *Adv. Energy. Mater.* **2011**, *1*, 1068.
[16] C. Meng, J. Maeng, S. W. M. John, P. P. Irazoqui, *Adv. Energy. Mater.* **2014**, *4*, 1301269.
[17] M. Beidaghi, C. L. Wang, *Electrochim. Acta* **2011**, *56*, 9508.
[18] N. Kurra, M. Hota, H. N. Alshareef, *Nano Energy* **2015**, *13*, 500.
[19] W. Gao, N. Singh, L. Song, Z. Liu, A. L. M. Reddy, L. Ci, R. Vajtai, Q. Zhang, B. Wei, P. M. Ajayan, *Nat. Nanotechnol.* **2011**, *6*, 6.
[20] M. F. El-Kady, R. B. Kaner, *Nat. Commun.* **2013**, *4*, 1475.
[21] J. Lin, Z. Peng, Y. Liu, F. Ruiz-Zepeda, R. Ye, E. L.G. Samuel, M. J. Yacaman, B. I. Yakobson, J. M. Tour, *Nat. Commun.* **2014**, *5*, 5714.
[22] L. Fan, N. Zhang, K. Sun, *Chem. Commun.* **2014**, *50*, 6789.
[23] H. Hu, K. Zhang, S. Li, S. Ji, C. Ye, *J. Mater. Chem. A* **2014**, *2*, 20916.
[24] I. D. van der Werf, G. Germinario, F. Palmisano, L. Sabbatini, *Anal. Bioanal. Chem.* **2011**, *399*, 3483.
[25] W. D. Mazzella, P. Buzzini, *Forensic Sci. Int.* **2005**, *152*, 241.
[26] A. Russo, B. Y. Ahn, J. J. Adams, E. B. Duoss, J. T. Bernhard, J. A. Lewis, *Adv. Mater.* **2011**, *23*, 3426.
[27] Y. Fu, X. Cai, H. Wu, Z. Lv, S. Hou, M. Peng, X. Yu, D. Zou, *Adv. Mater.* **2012**, *24*, 5713.
[28] S. E. J. Bell, S. P. Stewart, Y. C. Ho, B. W. Craythorneb, S. J. Speers, *J. Raman Spectrosc.* **2013**, *44*, 509.
[29] P. Subramanian, N. Clark, B. Winther-Jensen, D. MacFarlane, L. Spiccia, *Aust. J. Chem.* **2009**, *62*, 133.
[30] Y. G. Zhu, Y. Wang, Y. Shi, J. I. Wong, H. Y. Yang, *Nano Energy* **2014**, *3*, 46.
[31] K. Wang, H. Wu, Y. Meng, Z. Wei, *Small* **2014**, *10*, 14.
[32] D. J. Lipomi, R. V. Martinez, L. Cademartiri, G. M. Whitesides, in *Polymer Science: A Comprehensive Reference,* Vol. 7 (Eds: K. Matyjaszewski, M. Möller), Elsevier, Oxford, UK **2012**, pp. 211–231.
[33] S. Patra, N. Munichandraiah, *J. Appl. Polym. Sci.* **2007**, *106*, 1160.
[34] G. Cai, J. Tu, D. Zhou, J. Zhang, Q. Xiong, X. Zhao, X. Wang, C. Gu, *J. Phys. Chem. C* **2013**, *117*, 15967.
[35] W. Chen, R. B. Rakhi, L. Hu, X. Xie, Y. Cui, H. N. Alshareef, *Nano Lett.* **2011**, *11*, 5165.
[36] I. Horcas, R. Fernández, J. M. Gómez-Rodríguez, J. Colchero, J. Gómez-Herrero, A. M. Baro, *Rev. Sci. Instrum.* **2007**, *78*, 013105.

© 2015 WILEY-VCH Verlag GmbH & Co. KGaA, Weinheim